Long tail kinetics in biophysics?

John F. Nagle
Departments of Biological Sciences and Physics, Carnegie Mellon University, Pittsburgh, Pennsylvania 15213 USA

ABSTRACT Long tail kinetics describe a variety of data from complex, disordered materials that cannot be described by conventional kinetics. It is suggested that the kinetics of diffusive motion in complex biological media, such as cytoplasm or biomembranes, might also have long tails. The effects of long tail kinetics are investigated for two standard biophysical measurements, fluorescence recovery after photobleaching (FRAP), and dynamic light scattering (DLS). It is shown that long tail kinetic data would yield significantly distorted and misleading results when analyzed assuming conventional kinetics.

INTRODUCTION

From a variety of kinetic data measuring random motions of molecules in biological systems it has been customary to report diffusion constants D and immobile fractions f_{IM}. The theoretical basis for this analysis is the conventional diffusion equation:

$$D\nabla^2\rho(r, t) = \partial\rho/\partial t, \quad (1)$$

which has the usual Green's function (in one dimension):

$$P(x, t) = \exp(-x^2/4Dt)/(4\pi Dt)^{1/2}. \quad (2)$$

It has become increasingly clear for a variety of phenomena in a variety of fields that transport and diffusion are often not well represented by conventional diffusion (Eq. 1), especially for data from complex, disordered media, which are much better represented by long tail kinetics (1). Phenomenologically, long tail kinetics can be represented by a distribution function $\psi(t)$, which gives the probability of a molecule jumping at time t if it last jumped at time 0. A simple canonical form for $\psi(t)$ is

$$\psi(t) = \beta/(1 + t)^{1+\beta}, \quad (3)$$

where the parameter β must be greater than 0. Conventional diffusive behavior is obtained in the limit $\beta = \infty$; technically, one would replace Eq. 3 by $\psi(t) = \beta t^{-1-\beta}$ for $t > 1$ and $\psi(t) = 0$ for $t < 1$, but conventional behavior is also obtained when $\psi(t) = \exp(-t)$, which corresponds to a tail that falls off faster than any power of β in Eq. 3. In contrast, for $\beta < 1$ the kinetics are fundamentally different. In particular, there is no diffusion constant D! Indeed, transport coefficients in general depend upon the length and time scales of the experiment (1).

The possibility of long tail kinetics in biological systems arises because a diffusing probe molecule will visit a variety of different environments characterized by its relative proximity to various macromolecules or by caging of the probe in disordered arrangements of macromolecular structures. The kinetic time constant for movement from these different environments will be different and this will provide a continuous spectrum of trapping energies ϵ. This is one way that long tail kinetics can arise as is discussed by Scher et al. (1) who also give an insightful phenomenological formula for the parameter β. Their derivation assumes that the energy ϵ of the probe molecule is distributed, due to the variety of different environments, according to $\rho(\epsilon) \sim \exp(-\epsilon/kT_0)$, where T_0 is simply a temperature-like parameter characterizing the distribution. Then, the long tail parameter β is given by T/T_0, where T is the actual temperature. For an energy distribution that is narrower than a thermal Boltzmann distribution, $T/T_0 = \beta > 1$, one expects ordinary kinetics. However, long tail kinetics are expected when the probe energy distribution becomes broader than thermal, $T_0 > T$. Since differences in van der Waals energies of probes near different macromolecules are easily greater than kT, it seems likely, supposing an exponential energy distribution, that $T_0 > T$ and that long tail kinetics should be considered for biological systems.

The purpose of this paper is to examine whether long tail kinetics would make any significant difference in the interpretation of biophysical diffusion data as obtained by standard experimental methods. The focus of this paper is on the method of fluorescence recovery after photobleaching (FRAP) (2, 3). In particular, it is shown that analyzing long tail data, assuming the data conform to the normal diffusion equation, leads to the nonsensical result that values of D and f_{IM} vary widely as the space and time windows of the experiment are varied. Dynamic light scattering (DLS) (4) is also investigated and it is shown that the standard procedure for extracting a coefficient of diffusion D is also invalid for this method of measurement when the data have long tail kinetics.

RESULTS

Fig. 1 shows the FRAP signal $F(t)$ for long tail kinetics and for conventional diffusive kinetics. The signal $F(t)$ in Fig. 1 takes the value $F(0) = 0$ at time 0 when all molecules in a strip of width L have been bleached, and it takes the value $F(\infty) = 1$ when molecules from outside the bleached strip have repopulated the strip. Fig. 1

0006-3495/92/08/366/05 $2.00

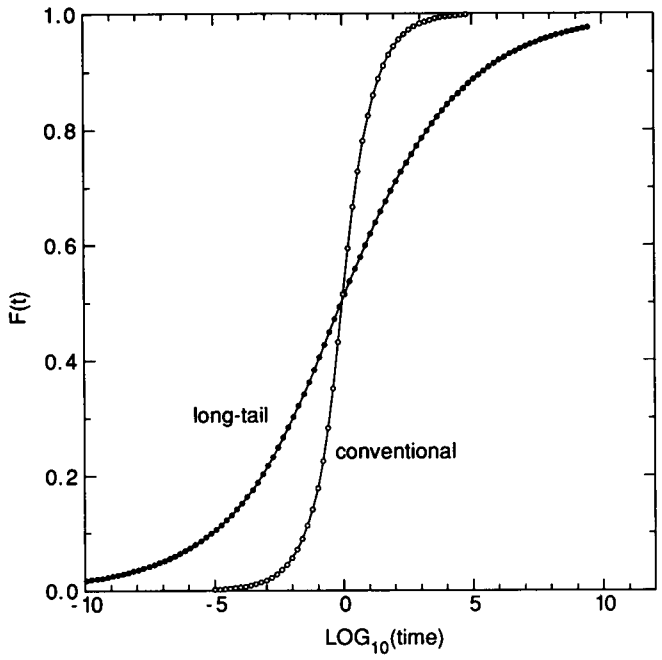

FIGURE 1 FRAP signal, $F(t)$, versus log(time). Comparison of conventional diffusive kinetics and long tail kinetics ($\beta = 0.3$).

shows that the FRAP signal is greatly stretched in time compared to the FRAP signal for conventional diffusion.

Fig. 2 shows the best fit, using conventional diffusive kinetics and assuming that there is an immobile fraction, to a portion of the data in Fig. 1. With good data over three decades of time it should be possible to diagnose long tail kinetics by the systematic deviations shown in Fig. 2. However, with no alternative theory one might

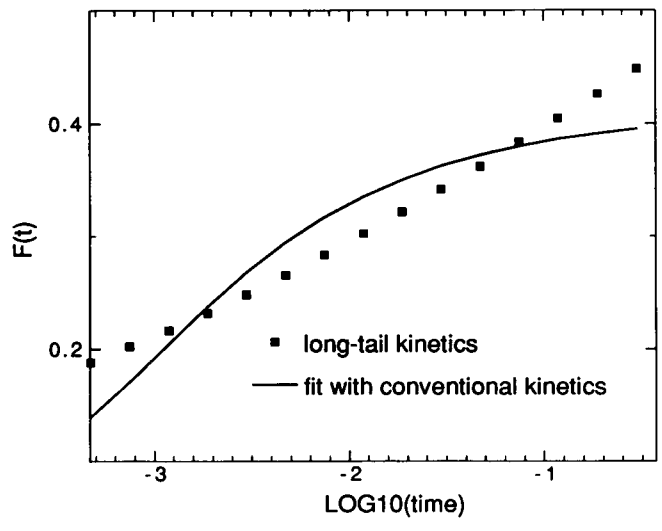

FIGURE 2 Three decades of the long tail data in Fig. 1 are shown by solid squares. The solid curve shows the best fit using conventional diffusive kinetics with immobile fraction $f_{IM} = 0.59$.

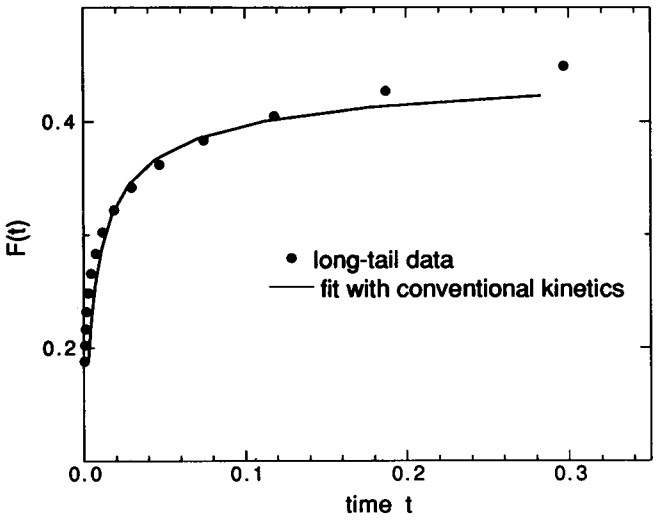

FIGURE 3 The solid circles show the same long tail data as in Fig. 2 versus linear time. The solid curve shows a visually appealing fit using conventional diffusive kinetics. The systematic errors in the fit are at the 3% level.

feel comfortable reporting f_{IM} and D values from the fit to the same data shown in Fig. 3. This latter fit is not as good as the fit in Fig. 2, but use of a linear instead of a log scale for the time obscures systematic deviations and allows a visually more pleasing fit. Table 1 shows the values of $f_M = 1 - f_{IM}$ and D that are obtained by fitting different portions of the long tail kinetics data in Fig. 1. The last column of Table 1 lists the systematic error σ of the fit. If there were additional random noise at the same level ($\sim$3%) as the systematic error σ, it would be even more difficult to see the systematic errors in Figs. 2 and 3.

Table 1 emphasizes that the fitted coefficient of diffusion D decreases dramatically as the time window is shifted to later times. This is typical behavior for long tail kinetics, which really do not have a constant coefficient of diffusion. The reason for the comparatively good fit is that the values of mobile fraction f_M also vary dramatically with the time window being fit by conventional diffusive kinetics.

TABLE 1 Best fit values of mobile fraction f_M and coefficient of diffusion D to long tail kinetics in Fig. 1 with time windows beginning at $t1$ and ending at $t2$

log ($t1$)	log ($t2$)	f_M	D/D_0	Sigma
−9.3	−6.3	0.0535	640,000	0.005
−6.3	−3.3	0.157	640	0.014
−3.3	−0.3	0.410	1.00	0.031
−0.3	2.7	0.708	0.0047	0.029
2.7	5.7	0.886	0.000031	0.014

The sigma of the fit is given in the last column. The apparent coefficients of diffusion D are normalized to the value D_0 in the middle time interval.

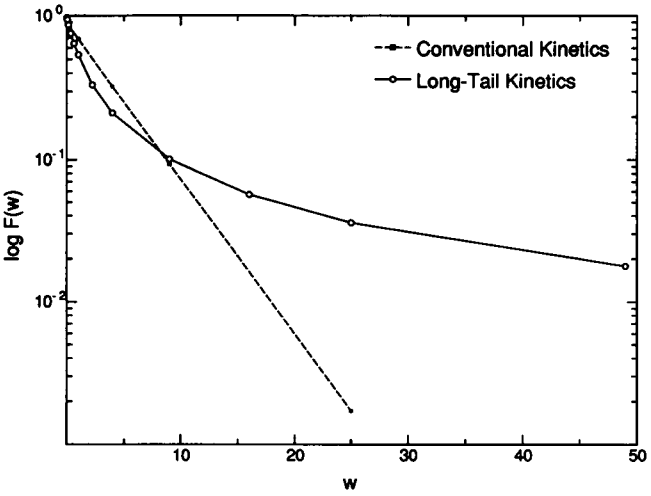

FIGURE 4 Dynamic light scattering self-intermediate scattering function $F(w)$ as a function of $w = q^2t^\alpha$, with $\alpha = 1$ for conventional kinetics and $\alpha \sim 0.31$ for long tail kinetics with $\beta = 0.3$.

It is equally interesting that if the space window (width L of the bleached strip in the FRAP experiment) is increased by a factor of r, while keeping the time window the same, the new values of D/D_0 and f_M are again given by Table 1, but after scaling the time window by a factor of $r^{-4.5}$. This means that increasing spot size in FRAP measurements will cause an apparent increase in D/D_0 and an apparent decrease in f_M if the kinetics have long tails.

Turning to dynamic light scattering, Fig. 4 shows the behavior of the self-intermediate scattering function $F(w)$ (4). For conventional diffusion, the variable w is q^2t and $F(w) = \exp(-wD)$, so that D may be obtained by the slope of the line in Fig. 4. In contrast, for long tail kinetics with $\beta = 0.3$, w is proportional to q^2t^α, with $\alpha \sim 0.31$, and for large w, $F(w)$ decays only algebraically as $w^{-\gamma}$ with $\gamma \sim 1.02$. As seen in Fig. 4, $\log [F(w)]$ for long tail kinetics does not have a constant slope so that attempts to extract D by fitting the data to a straight line will yield a different D depending upon the range of the data that are fit.

CALCULATIONS

The basic Green's function $P(x, t)$ for long tail kinetics can be written as

$$P(x, t) = \sum_{n=0}^{\infty} G_n(x)P_n(t). \quad (4)$$

The index n is the number of times molecules have hopped in time t, and $P_n(t)$ is the probability that molecules have hopped n times in time t. The mean hopping distance is taken to be 1. For molecules that have hopped n times, starting at $x = 0$, the probable spatial distribution is given by the usual Gaussian approximation to the binomial distribution:

$$G_n(x) = \exp(-x^2/2n)/(2\pi n)^{1/2}. \quad (5)$$

The standard random walk Green's function for one-dimensional diffusion given in Eq. 2 follows from Eqs. 4 and 5 by assuming that $P_n(t)$ is a delta function located at $n = 2Dt$. This means that the number of hops increases linearly with time. The only difference in long tail kinetics is that the form of $P_n(t)$ is considerably different. The other features of standard random walk theory, namely the mean hopping length and the Gaussian form for $G_n(x)$, are used in the same way as in the conventional theory.

The hopping Green's function, $P_n(t)$, was estimated using Monte-Carlo simulations. A uniform distribution, $p(y) = 1$, $y \in [0, 1]$, was generated pseudorandomly by a standard Monte-Carlo algorithm. The time t to the next hop was calculated by $1 + t = 1/y^{1/\beta}$. Since the probability ψ satisfies $\psi(t)dt = -p(y)dy$, $\psi(t)$ is given by Eq. 3. This method was also used to simulate classical kinetics, where $\psi(t)$ is given by $\exp(-t)$ by taking $t = -\ln(y)$. In this latter case, $P_n(t)$ has a maximum at $n = t$ with a width that grows only as $n^{1/2}$, so that on a relative time scale $P_n(t)$ effectively becomes a delta function at large time. In strong contrast, $P_n(t)$ for $\beta = 0.3$ has its maximum at $n = 0$ for all simulated times as shown in Fig. 5. This means that the most probable number of hops remains zero. However, as time increases, there are fewer and fewer molecules that have not hopped, $P_0(t) = (1 + t)^{-\beta}$, as expected from Eq. 3.

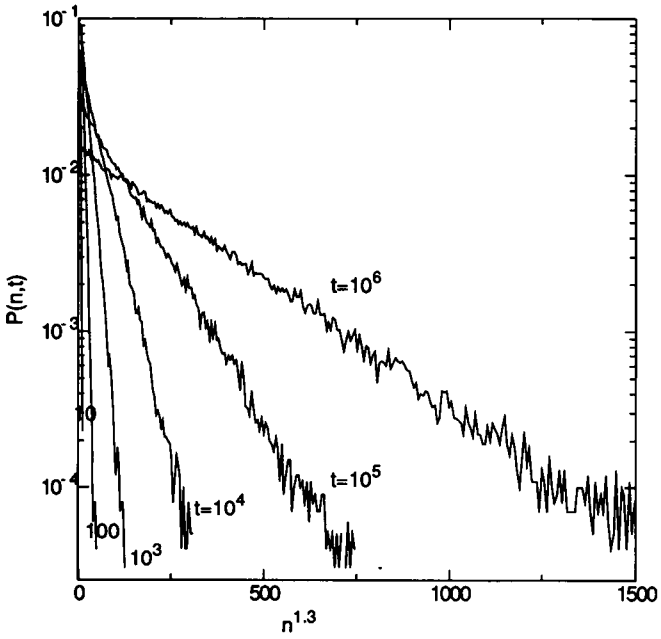

FIGURE 5 Simulations for the hopping Green's function $P_n(t)$ versus number of hops n to the power 1.3 for $\beta = 0.3$ for times $t = 10^m$, $m = 1 \ldots 6$. The number of hopping histories was 10^5.

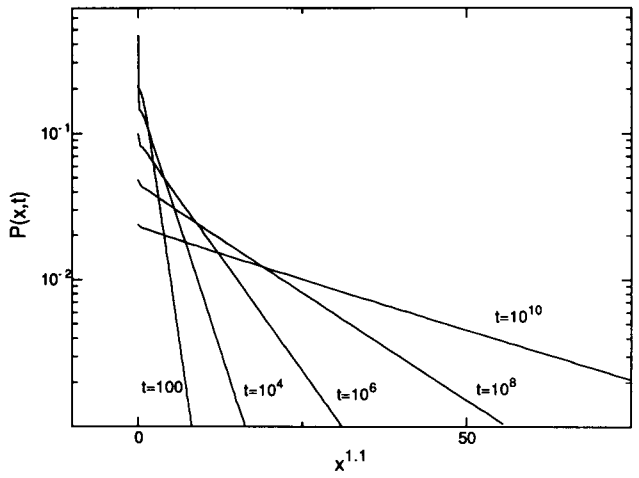

FIGURE 6 Calculations of the Green's function $P(x, t)$ versus distance x to the power 1.1 for $\beta = 0.3$ for times $t = 10^{2m}$, $m = 1 \ldots 5$.

Empirically, the simulated values of $P_n(t)$ are well approximated by straight lines when log P is plotted versus $n^{1+\beta}$ as shown in Fig. 5. Since $P_0(t) = (1 + t)^{-\beta}$, this means that $P_n(t)$ may be approximated as

$$P_n(t) \approx \exp(-[cn]^{1+\beta}/t^{\beta(1+\beta)})/t^{\beta}, \tag{6}$$

where c is chosen to normalize the distribution: for large t, $c = \Gamma(2 + \beta/1 + \beta)$. The approximate form in Eq. 6 clearly breaks down for larger β: for $\beta = 0.5$ the exponent of n has increased to ~ 1.9 instead of 1.5 and for $\beta = 0.7$ the maximum is not at $n = 0$.

Insertion of Eqs. 5 and 6 into Eq. 4 gives values of $P(x, t)$. Empirically, log $P(x, t)$ is remarkably linear as a function of $x^{1.1}$ as shown in Fig. 6. Although there is an anomalously large value at $x = 0$, this anomaly becomes smaller as t becomes larger. In addition, the slopes of the curves in Fig. 6 behave in a regular fashion as t is varied, decreasing by a factor of ~ 2.2 as t increases by 100. These regularities can be approximated by the following normalized form:

$$P(x, t) \approx 0.0104t^{-0.155} \exp(-0.014x^{1.1}/t^{0.17}). \tag{7}$$

Comparing this approximate form for $\beta = 0.3$ with the conventional Green's function in Eq. 2 highlights some major differences. First, the x dependence has changed from x^2 to $x^{1.1}$, as is emphasized in Fig. 6. Second, the t dependence is much slower with $t^{0.17}$ behavior in the exponential instead of t^1.

The signal in Fig. 1 was computed approximately using Eq. 7. The photoactivated (bleached) strip was taken to have length $2L = 1{,}000$, where the basic length unit is $x = 1$ and a normalized Green's function was centered at each of the 1,000 values of x in the strip. The FRAP signal is then given by

$$F(t) = 1 - \sum_{x=-L}^{L} \sum_{x'=-L-x}^{L-x} P(x', t). \tag{8}$$

The FRAP signal for ordinary diffusive kinetics was also calculated in the same way, except that Eq. 2 was used for $P(x, t)$ instead of Eq. 7.

The dynamic light scattering self-intermediate scattering function $F(w)$ is the spatial Fourier transform of $P(x, t)$ (Berne and Pecora, 1976), and the form in Eq. 7 was used in a numerical integration to obtain the result shown in Fig. 4.

The differences in the natural scaling for long tail kinetics and ordinary diffusive kinetics are revealed in Eqs. 2 and 7. For normal diffusive kinetics, increasing the length scale L by a factor of 10 results in an increase in the time required for 50% depletion by a factor of 100 because the scaling requires constant L^2/t_L in the exponential of Eq. 2. In contrast, for long tail kinetics, scaling in Eq. 7 requires constant $L^{1.1}/t_L^{0.17}$, so t_L scales as $L^{6.5}$. This scaling was employed in setting the time scale in Fig. 1 so that the FRAP signals change most rapidly near $t = 1$.

DISCUSSION

The specific result of this work is that long tail kinetics would substantially change the time course in the kinetics of biomolecular motion. This change could lead to confusing and suboptimal interpretation of experiments, such as FRAP experiments, as shown in the Results section. In particular, the reported coefficient of diffusion D and immobile fraction f_{IM} would depend upon the length and time scales of the measurement. This reflects the fact that long tail kinetics do not have diffusion constants and that the appearance of an immobile fraction would be due entirely to fitting an inappropriate theory to the data.

It should be emphasized again that the calculated example of long tail kinetics in this paper was solely for the value $\beta = 0.3$. For larger values of β up to 1, the differences between long tail kinetics and ordinary diffusive kinetics would be smaller but qualitatively similar.

The preceding paragraph emphasizes that β is an unknown phenomenological parameter that would be required to fit the theory to data. The other parameters that enter the theory set the length scale and the time scale, but the scaling relation mentioned at the end of the previous section shows that these are not independent variables and that only one additional independent parameter is required. Additionally, the length scale L of the experiment is required, for a total of three parameters. An appropriate combination of the parameters required could be the length scale L of the experiment divided by the mean hopping distance, the time scale for hopping and β. Conventional diffusive theory also requires three parameters, which are usually taken to be

the length scale L of the experiment, the coefficient of diffusion D, and the immobile fraction f_{IM}. Therefore, the long tail theory cannot be discriminated against on the grounds of parametric proliferation.

The conventional model consisting of two distinct populations of probe molecules, one fraction f_{IM} that is completely immobile and the other fraction f_M that is completely mobile, with no exchange between the fractions, is clearly an ideal one. The conventional model is appropriate in the case of strong chemical bonding of a fraction of the probe molecules to immobile structures. However, for physical interactions of the probe molecules with a fluctuating and disordered host environment, immobilization would never be complete and the extent of immobilization would constitute a continuous spectrum that would be best represented by long tail kinetics. It would seem appropriate that long tail kinetics be considered when analyzing kinetic data for diffusive motion in biological systems.

Both the conventional diffusive kinetic theory and the long tail kinetic theory are phenomenological theories. Both have an equally good base in random walk theory. More specific theory, necessary for evaluating the parameter β theoretically, involves modeling the details of each system and doing arduous model specific calculations, perhaps involving random walks in a disordered and/or percolating network (5). Meanwhile, the kind of random walk theory presented here could be useful to diagnose from experiments whether unconventional kinetics, such as represented phenomenologically by long tails, occur in biological systems.

Received for publication and in final form 9 December 1991.

REFERENCES

1. Scher, H., M. F. Shlesinger and J. T. Bendler. 1991. Time-scale invariance in transport and relaxation. *Physics Today.* 26–34.
2. Axelrod, D., D. E. Koppel, J. Schlessinger, E. Elson, and W. W. Webb. 1976. Mobility measurement by analysis of fluorescence photobleaching recovery kinetics. *Biophys. J.* 16:1055–1069.
3. Jacobson, K., Z. Derzko, E. Wu, Y. Hou, and G. Poste. 1976. Measurement of the lateral mobility of cell surface components in single, living cells by fluorescence recovery after photobleaching. *J. Supamol. Struct.* 5:8357–8362.
4. Berne, B. J., and R. Pecora. 1976. Dynamic Light Scattering. John Wiley and Sons, New York. 376 pp. See especially, 57–59.
5. Saxton, M. J. 1992. Lateral diffusion and aggregation. *Biophys. J.* 61:119–128.